Instituto de Física
Universidade de São Paulo

BEAM TRANSPORT SYSTEM

V. P Likhachev[1)], A. Sherbakov [2)], J.D.T. Arruda-Neto[1),3)]

[1)] Experimental Physics Department, Physics Institute, University of Sao Paulo, SP, Brazil

[2)] Kharkov Institute of Physics and Technology, 1 Akademishna, 61, 108 Kharkov, Ukraine

[3)] University of Santo Amaro /UNISA, Sao Paulo, Brazil

Publicação IF - 1561/2003

BEAM TRANSPORT SYSTEM

V. P. Likhachev, A. Sherbakov, J.D.T. Arruda -Neto

I – INTRODUCTION

The future Microtron of the University of São Paulo consists of a cascade of two racetrack microtrons with a maximum energy of 31 MeV. The accelerator uses room temperature accelerating structures in cw operation and should deliver an electron beam with 50 μA maximum current, 0.1% energy resolution and approximately 0.15π mm.mrad vertical and horizontal emittances.

The microtron beam is intended to be used with a high resolution photon tagging system in photonuclear experiments. Since the expected count rates in the nuclear reaction product arm will be rather small, about 100 counts per hour or less, due to the tagged photon flux limitations and very small cross section [1], the background in the experimental hall in the basement, 2.68 m below the accelerator hall must be as low as possible. Moreover, the beam at the spectrometer entrance (radiator position) must have characteristics compatible with the strict requirements needed to produce a polarized photon beam by the double off-axis collimation method.

This paper is concerned with the beam transport system, from the microtron to the tagger and then to the beam dump.

II – THE BEAM OPTICS PROJECT

The magnetic optics of the beam transport system has been calculated with the "TRANSPORT" computer code, based on the characteristics of dipole and quadrupole magnets that could be easily homebuilt. The final lay-out of the transport system is shown in figure 1.

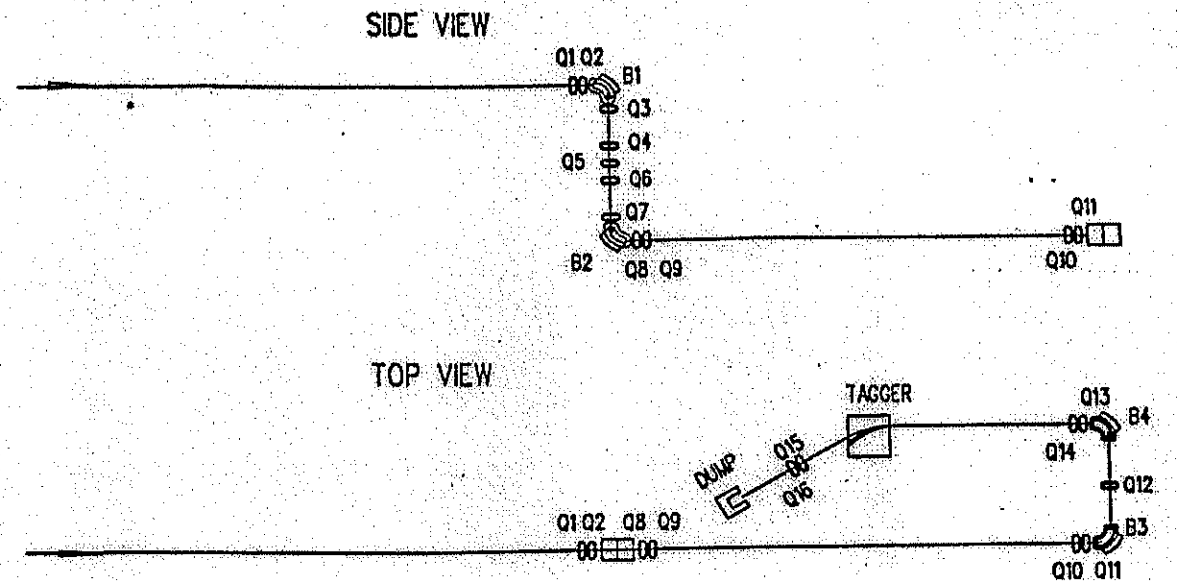

Figure 1 – Schematic view (top and side views) of the beam transport system.

The system can be divided in six functional parts:

1) Straight line from the accelerator to the first 90^0 bending magnet (SL-1);
2) Parallel shift (PS);
3) Sraight line from the second 90^0 bending magnet to the doubly achromatic 180^0 turn (SL-2);
4) Doubly achromatic 180^0 turn (U-turn);
5) Sraight line from the U-turn to the tagger magnet (SL-3);
6) Primary beam extraction system from the tagger to the beam dump or Faraday Cup (SE).

SL-1 consists of two quadrupoles Q_1 and Q_2 and has been designed to deliver the beam with suitable parameters for the parallel shift.

The achromatic PS has been designed to shift the beam from the horizontal level at the accelerator hall to the experimental hall 2.68 m below. This dispersionless system consists of two 90^0 bending magnets (B_1 and B_2) and five quaduproles (Q_3-Q_7), being symmetric around Q_5. This system can be used to reduce the emittance and energy spread of the beam by the introduction of slits or collimators in definite places along the trajectory, since the beam dimensions at those places are determined by either the energy spread or emittance. This question will be considered in detail in a forthcoming paper.

SL-2 consists of a horizontal focusing quadrupole (Q_8) and a quadrupole triplet (Q_9-Q_{11}) used to match the focus between the parallel shift and the U-turn.

The doubly achromatic (beam width and slope are independent of momentum at the image place [3] U-turn was designed using a lattice of two 90^0 bending magnets (B_3 and B_4) and quadrupole Q_{12}. The U-turn is needed to position the tagger in such a way that the primary beam will be directed to a bema dump placed in the labyrinth that leads to the old linac tunnel (see figure 2). The beam dump will be housed behind a 1 m thick concrete wall in order to improve background conditions in the experimental hall. Table 1 summarizes the parameters of the bending magnets.

SL-3 consists of two quadrupoles (Q_{13} and Q_{14}) and is used to provide, at the radiator position, the beam specification adequate for obtaining a polarized photon beam by the double off-axis collimation method in the tagger.

The extraction system, SE, consists of two magnets: i) spectrometer magnet (tagger) and ii) additional bending magnet. The additional bending magnet will have its field matched to the tagger magnet field in order to make the primary beam path after the tagger independent of the field setting in the tagger. In this way it will be possible to change the tagging energy interval and still keep the beam dump position fixed. Quadrupoles Q_{15} and Q_{16} are used to focus the beam after its passage through the radiator and tagger and additional magnet to the beam dump. This part of the calculation is the most complex, since after the interaction with the radiator the beam divergence increases and it is necessary to use second (or even higher) order approximation in the optics.

. Table 1 shows the characteristics of the magnetic lenses to be used.

QUADRUPOLES

Effective magnet length (m)	Field gradient (T/m)	Half-aperture (cm)
0.07	7.4	1.5

DIPOLES

Type	Effective magnet length (m)	Bend angle (degrees)	Entrance angle, pole-face rotation (degrees)	Exit angle, pole-face rotation (degrees)

B_1-B_4	0.4	90	0	0

Table 1 – Characteristics of the magnetic lenses

The operation regime of the magnetic elements for E_0=31 MeV is shown in table 2.

Magnetic element	Q_1	Q_2	B_1	Q_3	Q_4	Q_5
Position (m)	9.000	9.170	9.360	9.880	10.515	10.810
Field (T or T/m) (E_0=31 MeV)	-6.300	6.300	0.4061	7.367	-7.367	7.367

Magnetic element	Q_6	Q_7	B_2	Q_8	Q_9	Q_{10}
Position (m)	11.105	11.740	11.930	12.450	12.620	19.590
Field (T or T/m) (E_0=31 MeV)	-7.367	7.367	0.4061	-2.300	5.400	4.000

Magnetic element	Q_{11}	B_3	Q_{12}	B_4	Q_{13}	Q_{14}
Position (m)	19.760	19.930	21.030	21.800	22.300	22.470
Field (T or T/m) (E_0=31 MeV)	-4.000	0.4061	3.057	0.4061	-5.100	5.100

Table 2 – Parameters of the magnetic elements for E_0=31 MeV. The position parameter means the position at the entrance of the magnetic element.

The first order calculations for the beam envelope, divergence and dispersion are sown in figure 4-8. The second order calculations give practically the same results.

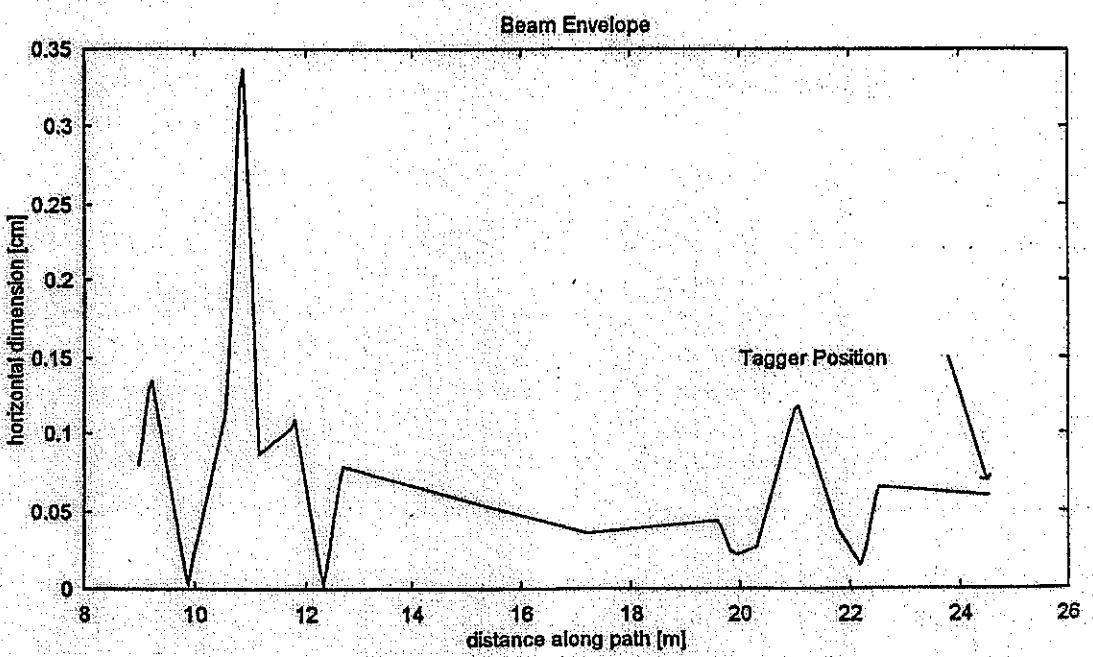

Figure 2 – Horizontal dimension (maximum half-width at the calculated points) of the beam along the path.

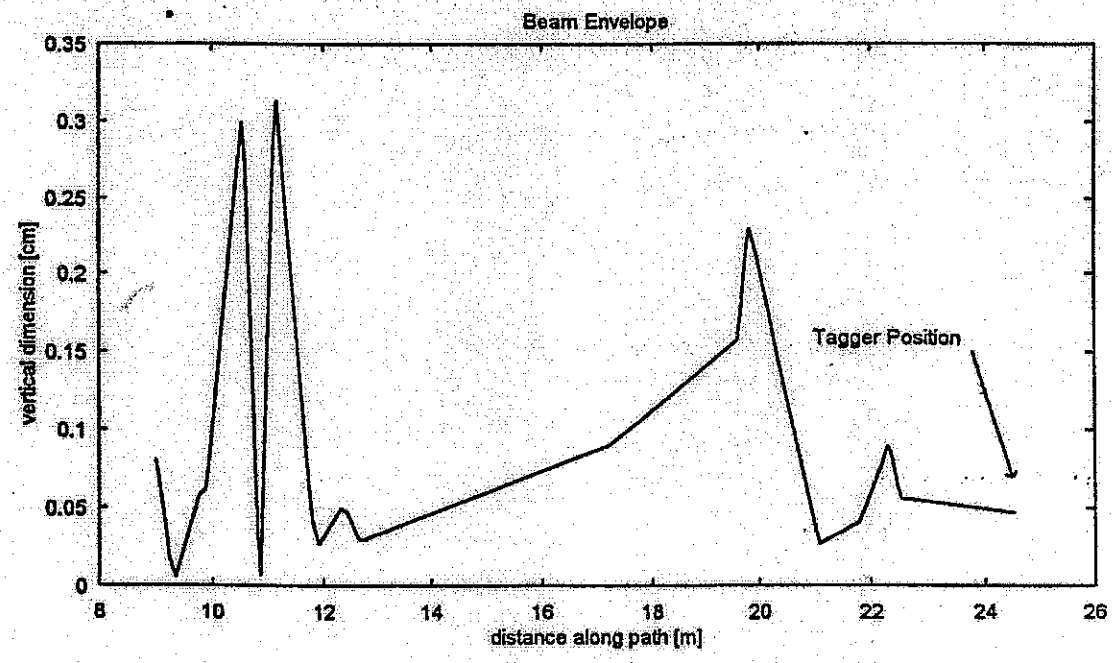

Figure 3 - Vertical dimension of the beam along the path (see caption of figure 2).

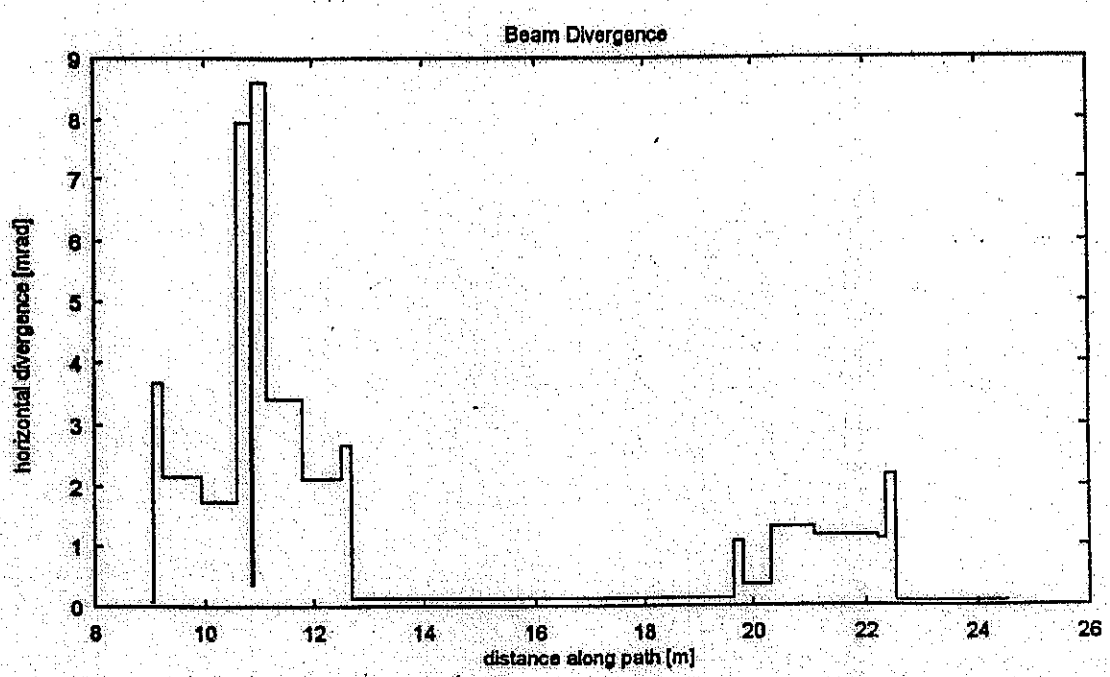

Figure 4- Horizontal divergence (maximum half-angular divergence of the beam envelope at the calculated points) of the beam along the path.

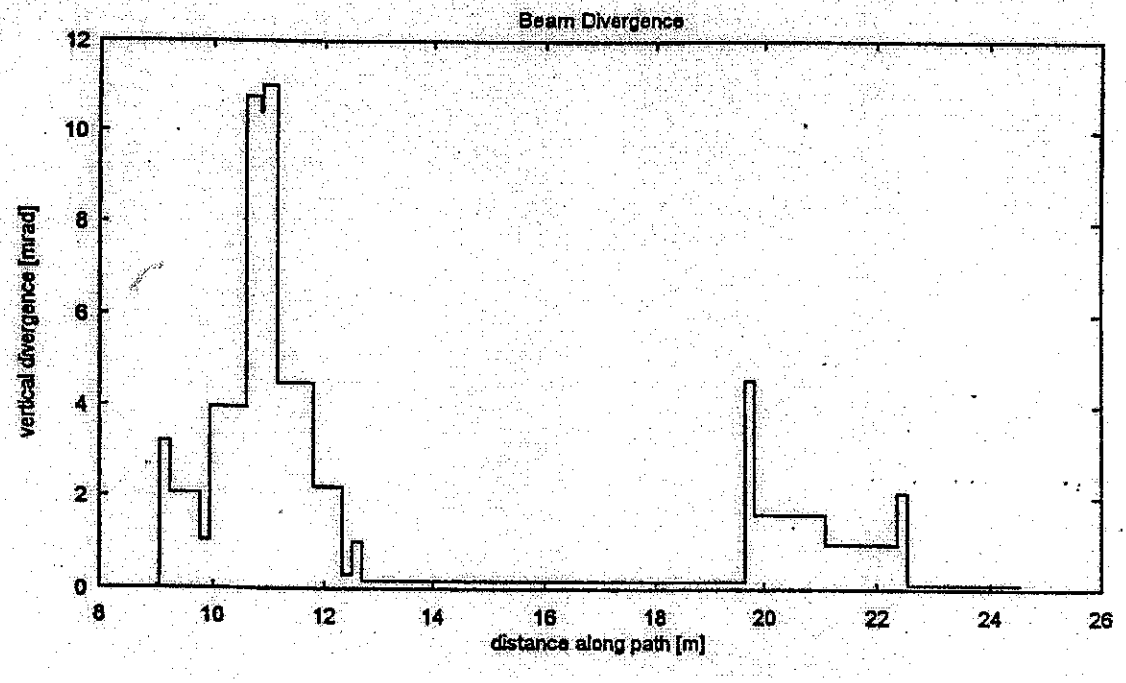

Figure 5 – Vertical divergence of the beam along the path (see caption of figure 4).

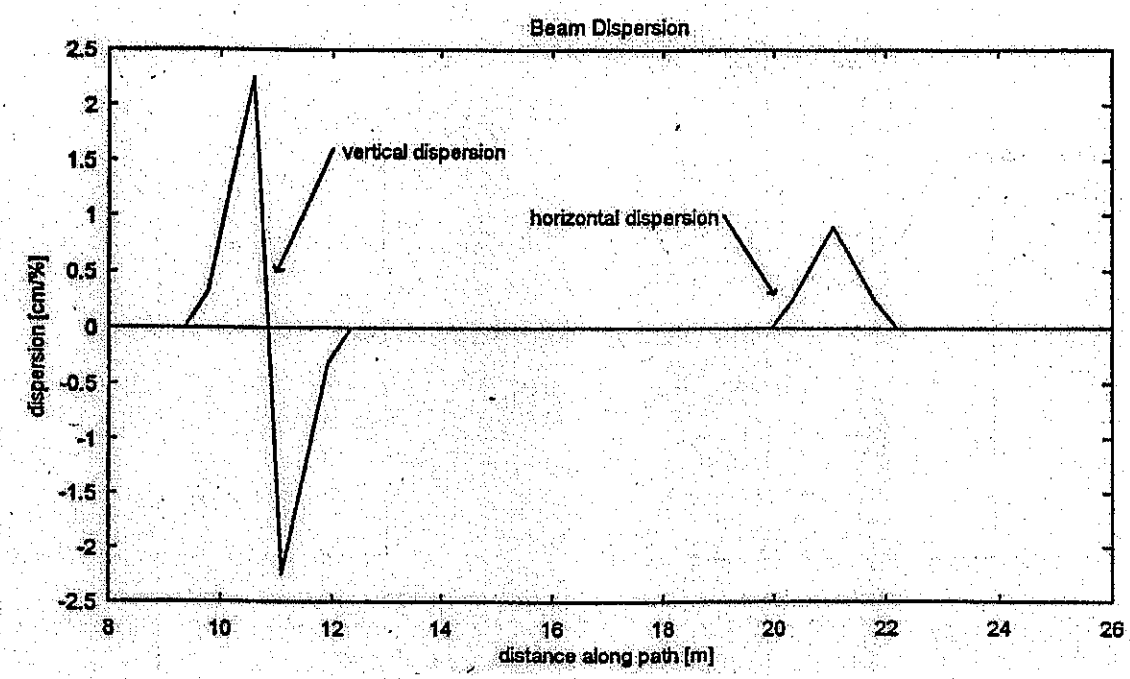

Figure 6 – Vertical and horizontal dispersions of the beam along the path. The region 11 m corresponds to the vertical dispersion (parallel shift), while the region around 21 m correspond to the horizontal dispersion (U-turn).

Figs 7 and 8 show top and side views of 90^0 band magnet used in the transport system (iron, coils).

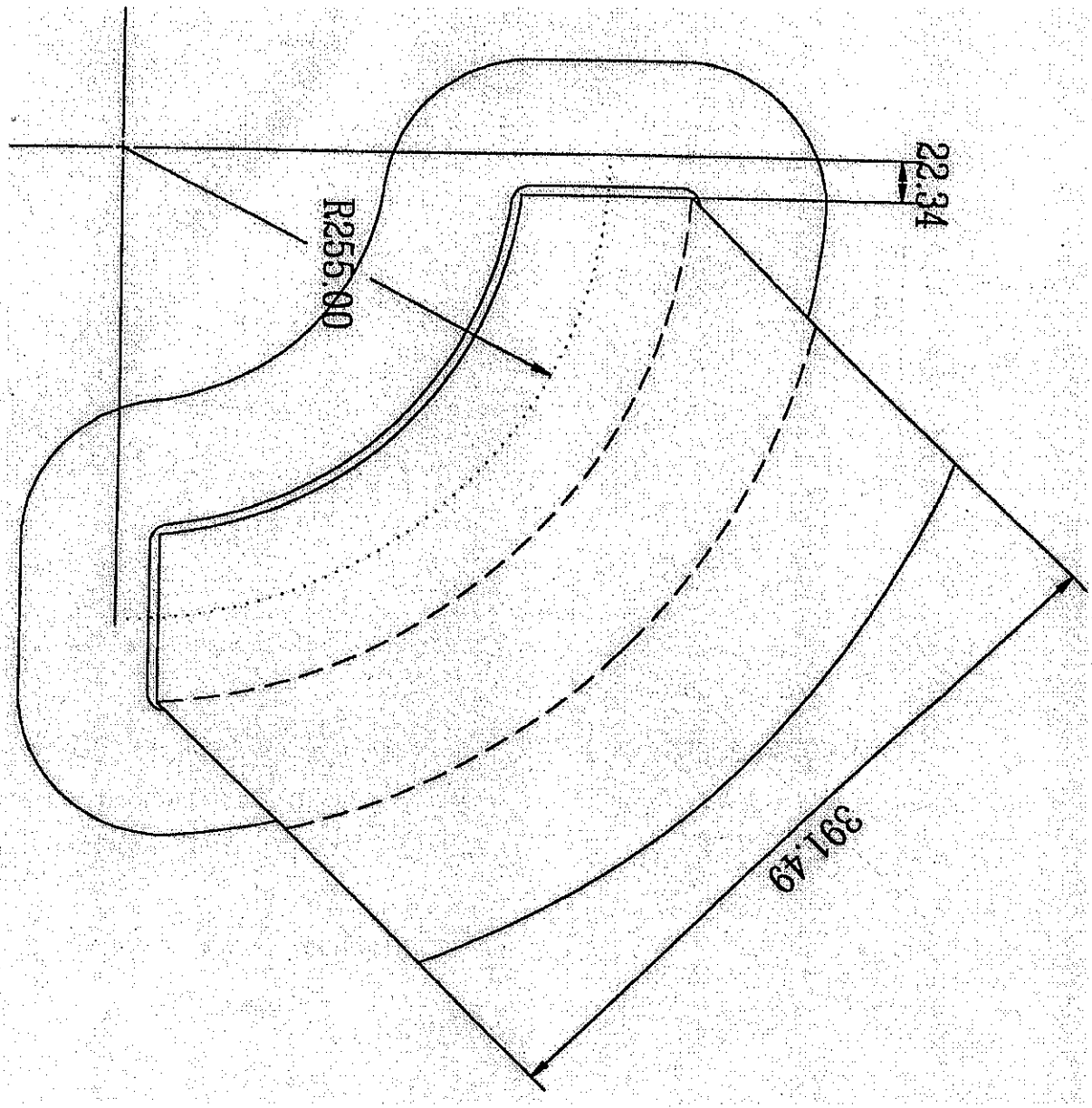

Figure 7. Top view of 90^0 band magnet (iron, coils)

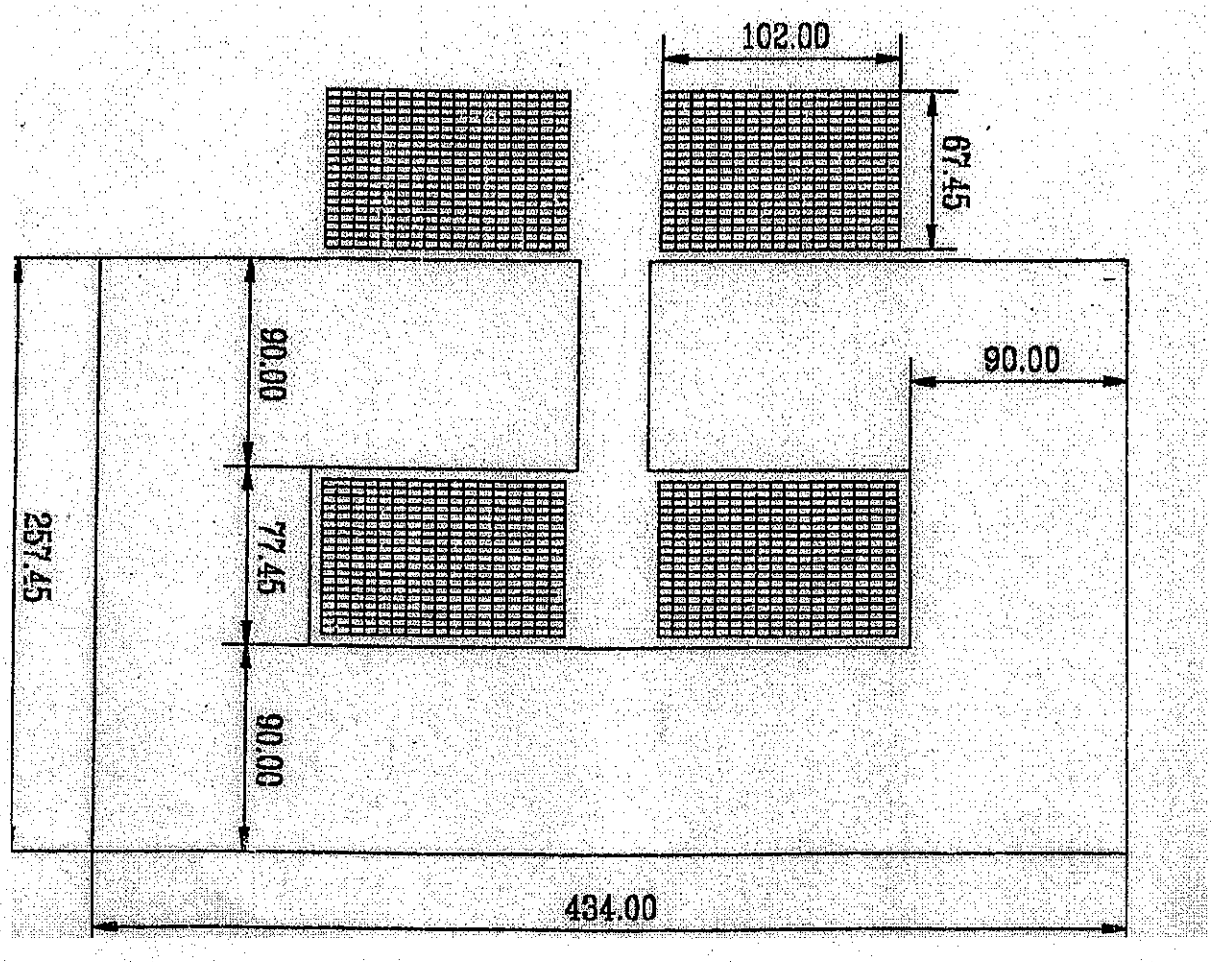

Figure 8. . Side view of 90^0 band magnet (iron, coils)

Figs 9 and 10 show the results of calculations of magnetic field uniformity inside the gap of 90^0 band magnet, which geometry is shown in figs 7 and 8.

The calculations were accomplished using the code "Poison".

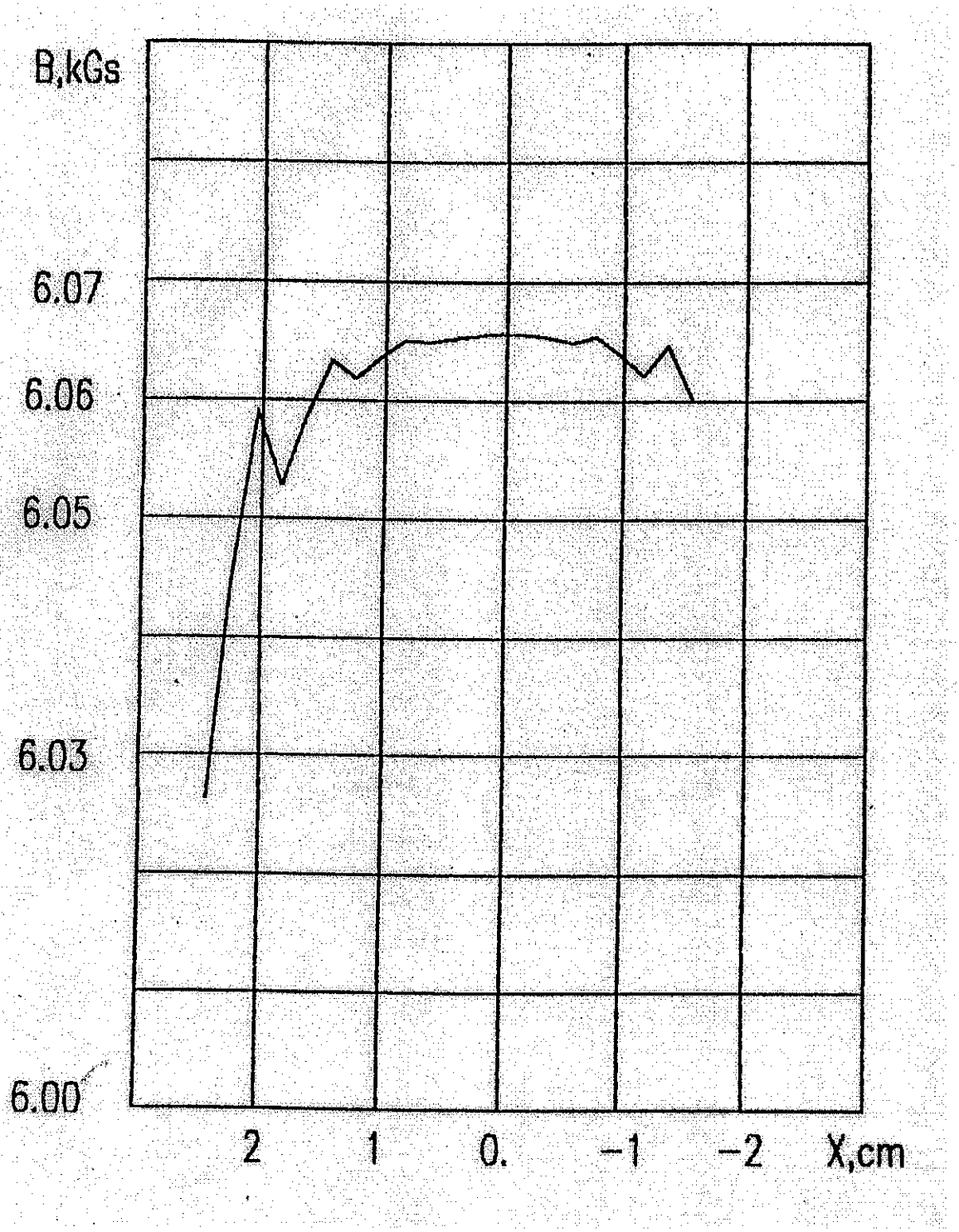

Figure 9. Calculated magnetic field uniformity inside 90^0 band magnet gap.

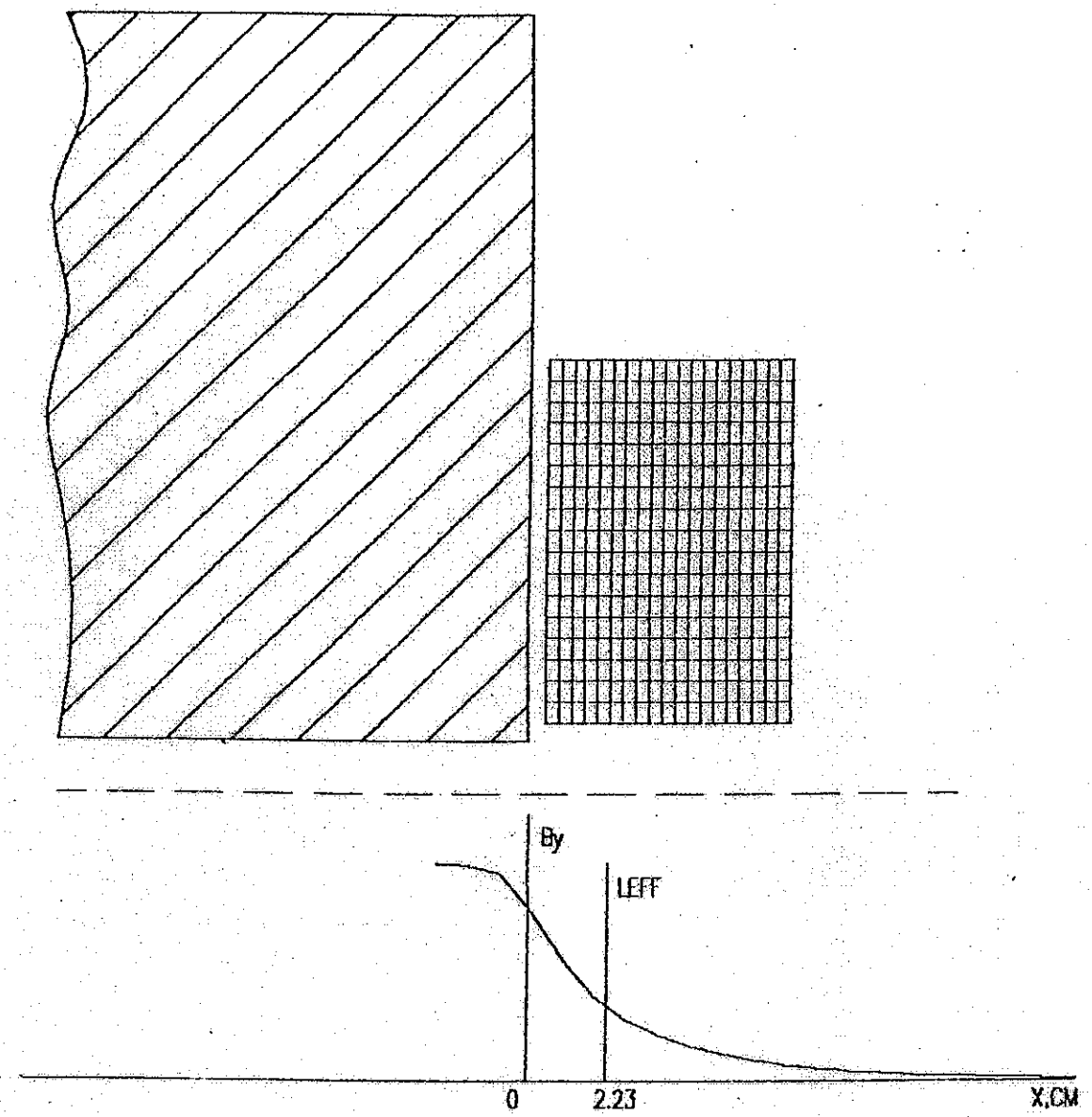

Figure 10. Edge effect and choice of the effective magnetic length for 90^0 band magnet gap.

REFERENCES

1. Disintegration of the deuteron by tagged, linearly-polarized photons: sensitivity of the differential cross section. V.P. Likhachev et al, Braz. J. of Phys. 27, 349 - 357 (1997)